Nucleon form factors from lattice QCD

Sara Collins
Universität Regensburg

11th International Workshop on Chiral Dynamics, RU Bochum, August 30th 2024

Nucleon form factors

Response of the nucleon to a probe:

Standard Model ($\gamma, W^{\pm}, Z$) or Beyond the Standard Model (??)

$\langle N'(p')|\mathbf{J}|N(p)\rangle = \bar{u}_{N'} \sum_i \kappa_i \mathbf{G_i(Q^2)} u_N$

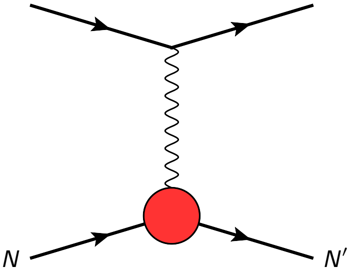

$N', N = p, n$. Local operator $\mathbf{J = J(0)}$. $\kappa_i = \kappa_i(\Gamma, p'_\mu, p_\mu)$.

$q = p' - p$, space-like region $-q^2 = Q^2 > 0$.

Lattice QCD: (results shown here) **work in isospin limit** $m_u = m_d$.

Reduced number of form factors in the Lorentz decomposition.

Nucleon form factors: information that can be extracted.

Neutral currents:

- $\boldsymbol{J = V}$, $G^{p,n}_{E,M} \to$ proton radius puzzle, $G^s_{E,M}(Q^2) \to$ parity-violating *ep* scattering experiments.
- $\boldsymbol{J = A}$, $G^q_A(Q^2 = 0) = g^q_A \to$ first moment of the helicity parton distribution function (PDF) $\to$ quark spin contribution to the spin of the nucleon.
- $\boldsymbol{J = T}$, $G^q_T(Q^2 = 0) \to$ first moment of the transversity PDF.
- $\boldsymbol{J = S}$, $m_q G^q_S(Q^2 = 0) \to$ nucleon sigma terms relevant for spin-independent WIMP-nucleon cross-section predictions.
- $\boldsymbol{J = \overline{q}\gamma_{\{\mu}\overleftrightarrow{D}_{\nu\}}q}$, generalised form factors $\to$ moments of generalised parton distribution functions $\to J_q = L_q + \frac{1}{2}g^q_A$ with $\frac{1}{2} = \frac{1}{2}\sum_q g^q_A + \sum_q L_q + J_g$. Gravitational form factors.

Charged weak currents:

- $\boldsymbol{J = A}$, $G_A(Q^2) \to$ input to predict the neutrino-nucleon scattering cross-section for long baseline neutrino oscillation experiments.
- $\boldsymbol{J = S, T}$, $G_S(Q^2 = 0) = g_S$ and $G_T(Q^2 = 0) = g_T \to$ searching for BSM signals in precision β decay experiments.

Not an exhaustive list.

EM and axial nucleon form factors

Neutral currents $(p \to p,\ n \to n)$: $V_\mu^q = \bar{q}\gamma_\mu q$, $A_\mu^q = \bar{q}\gamma_\mu\gamma_5 q$ with $q \in \{u, d, s, \ldots\}$

$$\langle N(p')|V_\mu^q|N(p)\rangle = \bar{u}_N(p')\left[F_1^q(Q^2)\gamma_\mu + \frac{F_2^q(Q^2)}{2m_N}\sigma_{\mu\nu}Q^\nu\right]u_N(p)$$

$$\langle N(p')|A_\mu^q|N(p)\rangle = \bar{u}_N(p')\left[G_A^q(Q^2)\gamma_\mu - i\frac{\tilde{G}_P^q(Q^2)}{2m_N}Q_\mu\right]\gamma_5 u_N(p)$$

Sachs ff.:

$$G_E^q(Q^2) = F_1^q(Q^2) - \frac{Q^2}{4m_N^2}F_2^q(Q^2), \quad G_M^q(Q^2) = F_1^q(Q^2) + F_2^q(Q^2)$$

with $\boldsymbol{J_\mu^{em} = \sum_q e_q V_\mu^q}$.

Charged currents $(n \to p)$: $\bar{u}\Gamma d$

Isospin limit $m_n = m_p$: $\langle p|\bar{u}\Gamma d|n\rangle = \langle p|\bar{u}\Gamma u - \bar{d}\Gamma d|p\rangle = \langle n|\bar{d}\Gamma d - \bar{u}\Gamma u|n\rangle$

Also: $\Gamma = \gamma_\mu$, $\quad \langle p|\bar{u}\gamma_\mu d|n\rangle = \langle p|J_\mu^{em}|p\rangle - \langle n|J_\mu^{em}|n\rangle$ etc..

EM and axial nucleon form factors

Forward limit, $Q^2 = 0$:

EM (vector neutral) current:

$$G_E^{\mathbf{p}}(0) = F_1^{\mathbf{p}}(0) = 1, \; G_M^{\mathbf{p}}(0) = F_1^{\mathbf{p}}(0) + F_2^{\mathbf{p}}(0) = \mu^{\mathbf{p}} = 1 + \kappa^{\mathbf{p}} = 2.79\ldots,$$

$$G_E^{\mathbf{n}}(0) = 0, \qquad G_M^{\mathbf{n}}(0) = \mu^{\mathbf{n}} = \kappa^{\mathbf{n}} = -1.91\ldots$$

Weak vector (charged) current: $G_E^{\mathbf{u-d}}(0) = G_E^{\mathbf{p-n}}(0) = 1,$
$G_M^{\mathbf{u-d}}(0) = G_M^{\mathbf{p-n}}(0) = \mu^{\mathbf{p-n}} = 4.70\ldots.$

Axial (neutral) current: $G_A^{\mathbf{q}}(0) = g_A^{\mathbf{q}}$

$\rightarrow$ quark spin contribution to the spin of the nucleon $\frac{1}{2} = \frac{1}{2}\sum_q g_A^q + \sum_q L_q + J_g$.

Weak axial (charged) current: $G_A^{\mathbf{u-d}}(0) \equiv G_A(0) = g_A^{\mathbf{u-d}} \equiv g_A$

Shape at low Q^2, $\langle r_X^2 \rangle = -\frac{6}{G_X(0)} \frac{dG_X(Q^2)}{dQ^2}$: different probe $\rightarrow$ different radius.

$$G_X(Q^2) = G_X(0)\left[1 - \frac{1}{6}\langle r_X^2 \rangle Q^2 + \ldots\right] \qquad X = E, M, A, P$$

Exception: $\langle r_E^2 \rangle^n = -6\frac{dG_E^n(Q^2)}{dQ^2}$

EM and axial nucleon form factors

Shape for larger Q^2: at present lattice up to ~ 1 GeV^2.

Phenomenological parameterisation:

e.g. dipole form, $G_A^{u-d}(Q^2) = G_A(Q^2) = g_A/(1+Q^2/M_A^2)^2$, $\langle r_A^2 \rangle = 12/M_A^2$.

Systematic approach: z-expansion [1008.4619,Hill,Paz].

$$G(Q^2) = \sum_{k=0}^{k_{max}} a_k z(Q^2)^k \qquad z(t, t_{cut}, t_0) = \frac{\sqrt{t_{cut}-t} - \sqrt{t_{cut}-t_0}}{\sqrt{t_{cut}-t} + \sqrt{t_{cut}-t_0}} \in \mathbb{R} \qquad t = -Q^2$$

Conformal mapping of the domain of analyticity onto the unit circle.
Polynomial expansion in z. Coefficients a_k are bounded in size, only a finite number are needed to describe the FF to a given precision.

$t_0 < 0$ is a tunable parameter.

For G_A, $t_{cut} = 9M_\pi^2$.

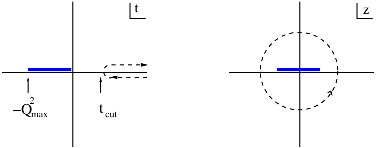

Lattice details: $\langle N|\bar{q}\Gamma q|N\rangle$

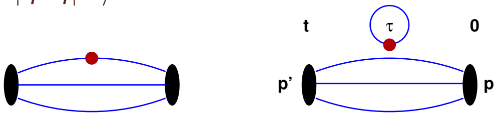

Isospin symmetric limit: Isovector $(u-d)$ combinations only connected quark-line diagrams.
Isoscalar (u,d,s,c) also disconnected: Methods used introduce additional stochastic noise.

Steps in the analysis:

Fit $C_{3pt,\Gamma_i}^{\vec{p}',\vec{p},J}(t,\tau) = \sum_{n,m} Z_n Z_m^* e^{-E_{\vec{p}'}^{n}(t-\tau)} e^{-E_{\vec{p}}^{m}\tau} \langle \boldsymbol{n(\vec{p}')|J|m(\vec{p})} \rangle \overset{t,\tau\to\infty}{\longrightarrow}$
$\sim e^{-E_{\vec{p}'}(t-\tau)} e^{-E_{\vec{p}}\tau} \langle \boldsymbol{N(\vec{p}')|J|N(\vec{p})} \rangle.$

Renormalisation to match lattice matrix element to a continuum scheme.

Repeat analysis on several ensembles to explore

- **Finite volume effects**: exponentially suppressed $\sim e^{-LM_\pi}$, $LM_\pi > 4$.
- **Cut-off effects**: $\mathcal{O}(a)$ or $\mathcal{O}(a^2)$, larger for larger $|\vec{p}|$, $|\vec{p}'|$.
- **Quark mass dependence**: chiral pert. theory (ChPT) $M_\pi \to M_\pi^{phys}$.

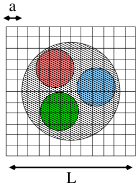

Cost of HMC
$\propto 1/(a^{\geq 6}\, m_\pi^{\approx 7.5})$

Also need Q^2 **parameterisation**: dipole, z-expansion, ...

Challenges in the baryon sector

Lattice provides (very) precise results for (see [FLAG21,2111.09849])
α_s, m_q, $q \in \{u/d, s, c, b\}$, $f_+^{K\to\pi\ell\nu}(q^2=0) = 0.9698(17)$, $f_K/f_\pi = 1.1932(21)$, ...

Baryon sector:

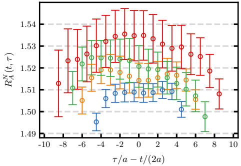

Statistical noise:
signal vs noise decays with $e^{-(E-3M_\pi/2)t}$ for large t.

$\rightarrow$ increase the number of "measurements" for large t.

Excited state pollution:
significant since t in $C_{3pt}^N(t,\tau)$ cannot be too large.

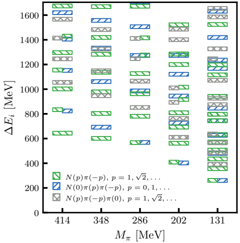

Contributions from resonances and **multi-particle states** — $N\pi$, $N\pi\pi$, ...

$M_\pi \rightarrow M_\pi^{phys}$: spectrum becomes denser ($LM_\pi \sim 4$), lowest states are multi-particle.

$\rightarrow$ e.g. [Mainz,2207.03440], 9-17 values of t in the range $t = 0.2 - 1.4$ fm.

Quark mass dependence: not clear how well ChPT describes the quark mass dependence in the range $M_\pi \sim (M_\pi^{phys} - 300\text{ MeV})$. Need $M_\pi \approx M_\pi^{phys}$.

Challenges in extracting the form factors

Extracting low Q^2 information:

Difficult to achieve low $Q^2 \neq 0$, (conventionally) $\rightarrow$ large L, $p_j = (2\pi n/L)$.

Extrapolation to reach $\tilde{G}_P(0)$ and $G_M(0) \rightarrow \mu$ and $\langle r_M^2 \rangle$.

Some radii are very sensitive to M_π: $\langle r_{E,M}^2 \rangle^{p-n}$ diverge as $M_\pi \rightarrow 0$.

Direct methods to determine $dG(Q^2)/dQ^2$: see, e.g.,

Momentum derivative method using moments of C_{3pt} in coordinate space [Aglietti et al.,hep-lat/9401004], used in [PACS,2107.07085]. See also [Bouchard et al.,1610.02354], and [ETMC,2002.06984,1605.07327].

Expansion of correlation functions with respect to the spatial components of external momenta [Divitiis et al.,1208.5914], used in [LHPC,1711.11385].

Also partially twisted boundary conditions to access smaller Q^2, see, e.g., [Divitiis et al.,hep-lat/0405002], [Sachrajda and Villadoro,hep-lat/0411033], applied in [QCDSF/UKQCD,Lattice 2008].

Not applicable to quark-line disconnected diagrams.

Electromagnetic form factors of the nucleon: $G_{E,M}^{p-n}$, $G_{E,M}^{p,n}$

Proton electric charge radius: $\langle r_E^2 \rangle^{1/2,p} = r_p$

Determined from:

Hydrogen spectroscopy, **muonic-hydrogen spectroscopy**, *ep* **scattering**.

[Xiong and Peng,2302.13818]

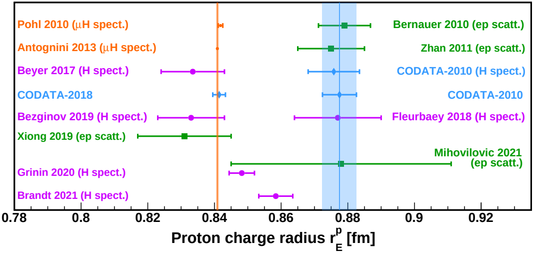

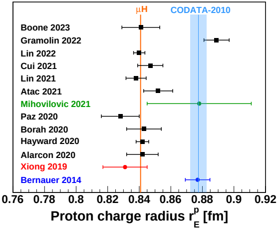

Right: re-analyses of *ep* scattering data.

Future/ongoing experiments: *ep* (MAGIX, PRad-II, ULQ2), μp (MUSE, AMBER), ...

MAGIX, Schlimmer, Tue 10:45.

Dispersive theory, Hammer, Wed 9:00.

Lattice: need results for $r_E^p = \langle r_E^2 \rangle^{1/2,p} < 2\%$ error with all systematics included!

Isovector EM form factors $G_{E,M}^{p-n}$

Only need to evaluate 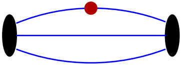 .

[NME,2103.05599] $N_f = 2+1+1$, $a = 0.13, 0.09, 0.07$ fm, $M_\pi = 166 - 285$, $LM_\pi^{min} = 4.3$.

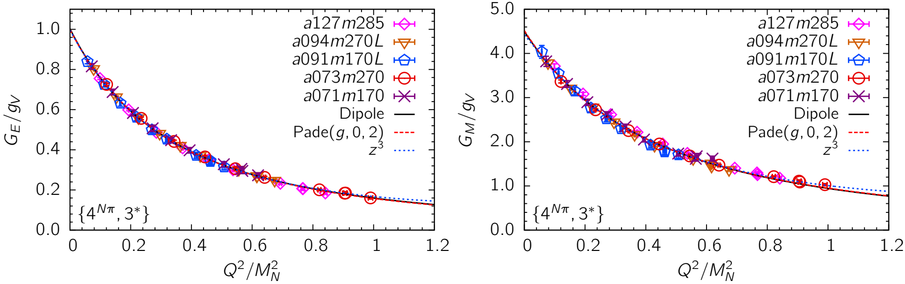

Q^2/M_N^2 instead of Q^2: observe milder cut-off effects.

Minimum $Q^2 \neq 0$ is 0.045 GeV^2.

Isovector EM form factors $G_{E,M}^{p-n}$

Fits to $G_{E,M}^{p-n}$ (■, □), direct determinations (○).

$Q^{2,min} \sim 0.04 - 0.06$ GeV^2, PACS 23 $L = 10.8$ fm, $Q^{2,min} = 0.015$ GeV^2. Different analyses.

PNDME20, NME21, Mainz21, Mainz23: several a, range of M_π, $LM_\pi \sim 4$.

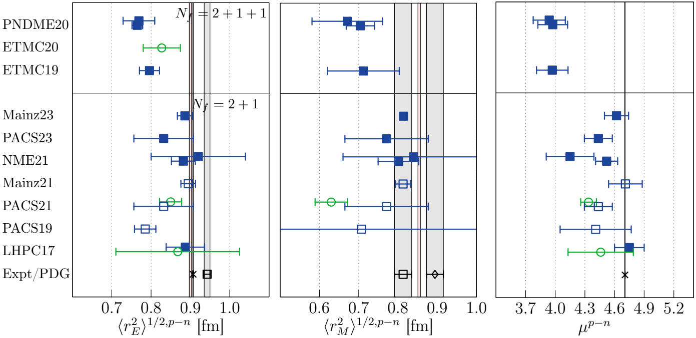

Experiment: following [Mainz,2309.06590]: $\mu^{p,n}$ (×), $\langle r_{E,M}^2 \rangle^n$ from PDG.

$\langle r_E^2 \rangle^p$: PDG (×), [A1,1007.5076] (□)

$\langle r_M^2 \rangle^p$: [Lee et al.,1505.01489] A1 at MAMI (□), World data excluding A1 (⋄).

Red: combined analysis of EM FF in time-like and space-like regions using dispersion theory [Lin et al.,2109.12961,2312.08694] "The proton magnetic radius: A new puzzle?"

EM form factors of the proton and neutron $G_{E,M}^{p,n}$

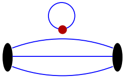

Need to also evaluate disconnected quark-line diagrams. Methods required introduce additional stochastic noise.

[Mainz,2309.06590,2309.07491] $N_f = 2+1$, $a = 0.09 - 0.05$ fm, $M_\pi = 130 - 290$ MeV, $LM_\pi \gtrsim 4$, utilise $Q^2 \lesssim 0.6$ GeV^2.

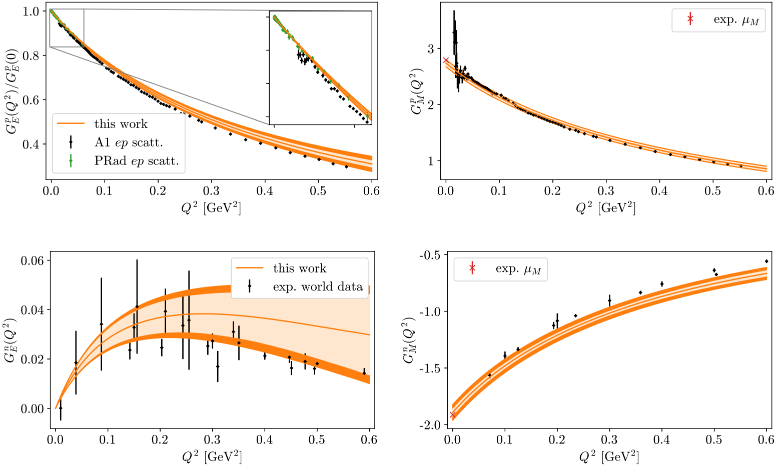

EM form factors

Mainz23: for each flavour combination $u-d$ and $u+d-2s$ fit $G_{E,M}$ together using $O(q^3)$ covariant baryon ChPT [Bauer et al.,1209.3872] EOMS + vector mesons but without Δ d.o.f.

Common LECs $\rightarrow$ much reduced uncertainty on μ, $\langle r_M^2 \rangle$ compared to independent z-expansion of G_E and G_M.

Only [Mainz,2309.06590] (This work) and ETMC19 (M_π^{phys}, $a = 0.08$ fm) include the disconnected contributions.

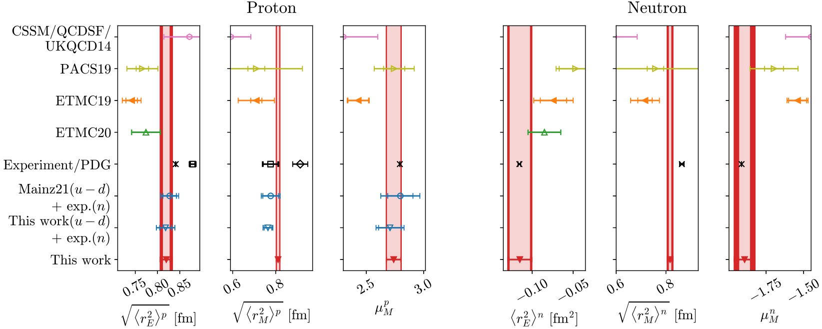

Total uncertainties: 2% for $\langle r_E^2 \rangle^{1/2,p}$, 1% for $\langle r_M^2 \rangle^{1/2,p}$, 2% for μ_M^p.

See also [Mainz,2309.17232] determination of the Zemach and Friar radi.

Axial form factors of the nucleon

Motivation: neutrino oscillation experiments

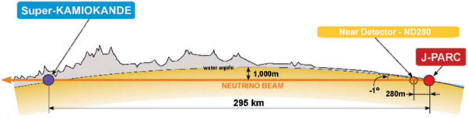

T2K: Tokai to Super-Kamiokande,

$E = 0.6$ GeV, $L/E \approx 500$ **km/GeV.**

Also NOvA, $L/E \approx 400$ km/GeV, DUNE $L/E \approx 520$ km/GeV, HK(=T2K).

Muon neutrino beam: proton on nucleus $\rightarrow$ pions and kaons $\rightarrow \mu^+\nu_\mu$ or $\mu^-\bar{\nu}_\mu$.

Near and far detectors.

$$\mathbf{N}^{\mu}_{\rm far}(\mathbf{E}_\nu) = \mathbf{N}^{\mu}_{\rm near}(\mathbf{E}_\nu) \times [\text{flux(L)}] \times [\text{detector}] \times [1 - \sum_\beta \mathbf{P}_{\mu\to\beta}(\mathbf{E}_\nu)]$$

E_ν has to be reconstructed from the momentum of the detected charged lepton.

$\nu_\mu + n \rightarrow \mu^- + p$

But. . .
The neutrino beam is not monochromatic but has a momentum distribution.
The nucleon is bound in a nucleus and has $|\mathbf{p}_{\rm Fermi}| \sim 200$ MeV.
The lepton momentum reconstruction is often incomplete.
Misidentification of inelastic scattering as elastic scattering.

Monte-Carlo simulation needs input regarding the differential cross section.

Neutrino-nucleon scattering cross-section

Quasi-elastic scattering (QE)

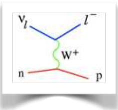

Resonance production (RES)

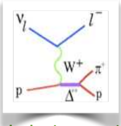

Deep Inelastic scattering (DIS)

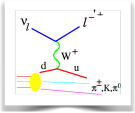

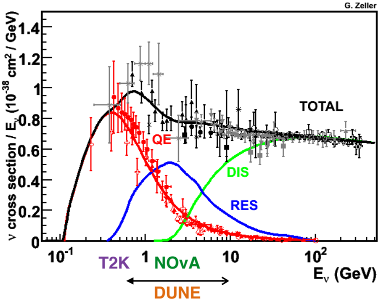

J.A. Formaggio, G. Zeller, Reviews of Modern Physics, 84 (2012)

14

First calculations of $N \to N\pi$ matrix elements [Barca et al.,2211.12278], [ETMC,2408.03893] (motivated by removing excited state contamination of $N \to N$).

$N \to$ resonance: $1 \to 2$ body finite volume formalism [Bernard et al.,1205.4642], [Agadjanov et al.,1405.3476], [Briceno, Hansen,1502.04314] also requires $N\pi \to N\pi$ scattering information. Scattering: Morningstar, Mon 10:45, Pittler, Mon 16:10.

Nuclear effects: Gnech, Tue 11:25, Piarulli, Tues 12:05.

Quasi-elastic scattering

Relevant $V - A$ matrix element in the isospin limit:

$$\langle \mathbf{p}(\mathbf{p}')|\bar{\mathbf{u}}\gamma_\mu(\mathbf{1}-\gamma_5)\mathbf{d}|\mathbf{n}(\mathbf{p})\rangle = \overline{u}_p(p')\left[\gamma_\mu \boldsymbol{F_1(Q^2)} + \frac{i\sigma_{\mu\nu}q^\nu}{2m_N}\boldsymbol{F_2(Q^2)} + \gamma_\mu\gamma_5 \boldsymbol{G_A(Q^2)} + \frac{q^\mu}{2m_N}\gamma_5 \boldsymbol{\tilde{G}_P(Q^2)}\right] u_n(p)$$

$q_\mu = p'_\mu - p_\mu$, virtuality $Q^2 = -q^2 > 0$.

Isovector Dirac and Pauli form factors $F_{1,2}$ are reasonably well determined experimentally from lepton-nucleon scattering for range of $Q^2 \sim (0.1 - 1)$ GeV^2 relevant for the long-baseline experiments.

$G_A(Q^2)$**:** information from old $\bar{\nu}$-p and ν-d scattering data.

Over-constrained dipole fits performed: $G_A(q^2) = \frac{g_A}{(1+\frac{q^2}{\mathbf{M_A}^2})^2}$, $M_A = 2\sqrt{3}/\langle r_A^2\rangle^{1/2}$.

e.g. [Bernard et al.,hep-ph/0107088] $M_A = 1.03(2)$ GeV.

z-expansion analysis from [Meyer,1603.03048] $M_A = 1.01(24)$ **GeV**.

Neutrino scattering with nuclear targets, e.g. [MiniBooNE,1002.2680] $M_A = 1.35(17)$ GeV (using the dipole form).

Axial and induced pseudoscalar form factors

$\tilde{G}_P(Q^2)$:

Impact on the cross section is suppressed by a factor $m_\ell^2/m_N^2 \approx 0.01$ for $\ell = \mu$.

Only relevant for very small Q^2, where this form factor is large.

Not well constrained: experimentally measured at the muon capture point. In muonic hydrogen, $\mu^- + p \to \nu_\mu n$.

[MuCAP, 1210.6545] : $g_P^* = m_\mu \tilde{G}_P(0.88 m_\mu^2)/(2m_N) = 8.06 \pm 0.48 \pm 0.28.$

Additional indirect information on G_A and $\tilde{G}_P$ via low energy theorems from pion electroproduction $e^- + N \to \pi + N + e^-$, see, e.g. [Bernard et al.,hep-ph/0107088].

PCAC relation and pion pole dominance

In the continuum limit, for nucleon matrix elements: $A_\mu = \bar{u}\gamma_\mu\gamma_5 d$, $P = \bar{u} i\gamma_5 d$,

$$\mathbf{2\, m_\ell} \langle p(\vec{p}\,')|\mathbf{P}|n(\vec{p})\rangle = \langle p(\vec{p}\,')|\partial_\mu \mathbf{A}_\mu|n(\vec{p})\rangle$$

$(m_u = m_d = m_\ell)$ leads to

$$m_\ell G_P(Q^2) = m_N G_A(Q^2) - \frac{Q^2}{4m_N}\tilde{G}_P(Q^2)$$

where the **pseudoscalar form factor**: $\langle p(p')|P|n(p)\rangle = \overline{u}_p i\gamma_5 \boldsymbol{G_P(Q^2)} u_n$.

SU(2) chiral limit: $\tilde{G}_P(Q^2) = 4m_N^2 G_A(Q^2)/Q^2$

Finite M_π^2, **pion pole dominance** (LO ChPT): only an approximation.

$$\tilde{G}_P(Q^2) = G_A(Q^2)\frac{4m_N^2}{Q^2 + M_\pi^2} + \mathrm{corrections}$$

PCAC+pion pole dominance (PPD) $\to$ only one independent form factor, e.g., $G_A(Q^2)$

$$G_P(Q^2) = G_A(Q^2)\frac{m_N}{m_\ell}\frac{M_\pi^2}{Q^2 + M_\pi^2} + \mathrm{corrections}$$

Excited state contamination in ChPT

$N\pi$ excited state contamination in correlation functions can be investigated in ChPT.

For example,

Forward limit (zero recoil):
[Tiburzi,0901.0657,1503.06329] $N\pi$ excited state contribution to $G_A(0) = g_A$ in leading loop order HBChPT.
[Hansen,1610.03843] $N\pi$ excited state contribution to g_A, LO ChPT with finite volume interaction corrections obtained from the experimental scattering phase a la Lellouch-Lüscher.
[Bär,1606.09385] BChPT: leading loop order g_A.

Form factors:
[Meyer,1811.03360] $N\pi$ contributions to $G_A(Q^2)$, $\tilde{G}_P(Q^2)$ and $G_P(Q^2)$ computed to tree-level in ChPT.
[Bär,1906.03652,1812.09191] $N\pi$ contributions to $G_A(Q^2)$, $\tilde{G}_P(Q^2)$ and $G_P(Q^2)$ computed in leading loop order BChPT.
[Bär,2104.00329] $N\pi$ contributions to $G_E(Q^2)$, $\tilde{G}_M(Q^2)$ computed in leading loop order BChPT.

Limitations to ChPT approach: pion momentum and M_π should be small. Applies to large source-sink separation (not always accessible due to deterioration of the signal). When using spatially extended sources $\langle r^2 \rangle_{smear}^{1/2} \ll 1/M_\pi$.

Excited state contamination in ChPT

Ground state: $N(-\vec{q}) \to N(\vec{0})$. $C^{\vec{p}',\vec{p},J}_{3pt,\Gamma_i}(t,\tau) = \sum_{n,m} Z_n Z_m^* e^{-E^n_{\vec{p}'}(t-\tau)} e^{-E^m_{\vec{p}}\tau} \langle \boldsymbol{n(\vec{p}')|J|m(\vec{p})} \rangle$.

Axial form factors

Axial and pseudoscalar currents can directly couple to pions: dominant contributions come from **tree-level diagrams**, where the pion takes the momentum of the current.

Large $N(\vec{0})\pi(-\vec{q}) \to N(\vec{0})$ and $N(-\vec{q}) \to N(-\vec{q})\pi(\vec{q})$ contributions for some combinations of the current and momentum transfer.

At tree-level only extraction of $\tilde{G}_P$ and G_P affected.

$N\pi$ contamination is largest as $M_\pi \to M_\pi^{phys}$ and low $Q^2 \neq 0$.

No enhanced excited state contributions to G_A.

$\to$ (moderate) loop contributions to $\mathcal{A}_i \perp \vec{q}_i$.

Consistent with lattice data.

Isovector electromagnetic form factors

No tree-level $N\pi \to N$ contributions. Excited state contamination from $N\pi$ is "moderate". $N\pi\pi \to N$ transition matrix elements not studied.

Forward limit: axial charge, $G_A(0) \equiv g_A$

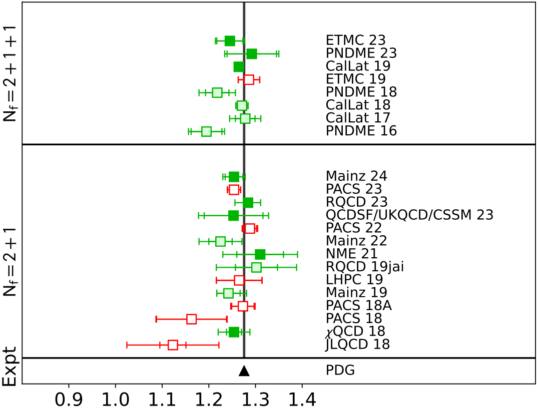

ETMC 23, PNDME 23, Mainz 22 and RQCD 19 results obtained from data for $Q^2 > 0$ as well as $Q^2 = 0$.

Rest: $Q^2 = 0$ only.

Recent results for $G_A(Q^2)$

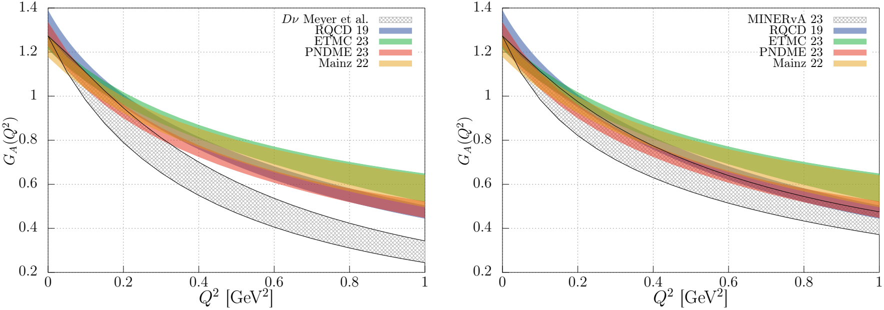

Shown: [RQCD,1911.13150], [Mainz,2207.03440], [PNDME,2305.11330], [ETMC,2309.05774].

All perform continuum, physical point $M_\pi \to M_\pi^{phys}$, finite volume extrapolations.

Left: νD fit from [Meyer et al.,1603.03048].
Right: $\bar{\nu} H$ fit from [MINERva,Nature 614, 48 (2023)]: antineutrino scattering off hydrogen atoms inside hydrocarbon molecules.

Fits to expt., $Q^2 = 0$ fixed using $G_A(0) = g_A$. Not the case for the lattice results.

See also, e.g., [NME,2103.05599], [CalLat,2111.06333], [PACS,2311.10345]

Axial radius: $\langle r^2 \rangle_A$ [fm^2]

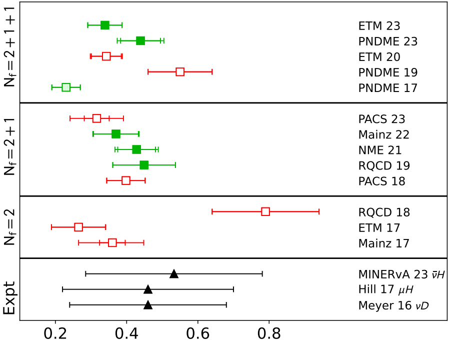

Lattice results and fits to experiment obtained using the z-expansion.

μH [Hill et al.,1708.08462]

Neutrino-nucleon cross-section

[Meyer et al.,2201.01839]

LQCD fit: [CalLat,2111.06333] $M_\pi = 130$ MeV, $LM_\pi = 3.9$, $a = 0.12$ fm.

Consistent with other lattice results but 1 ensemble, no continuum limit, only lattice data for $Q^2 < 1.2$ GeV^2.

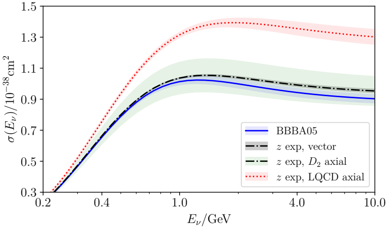

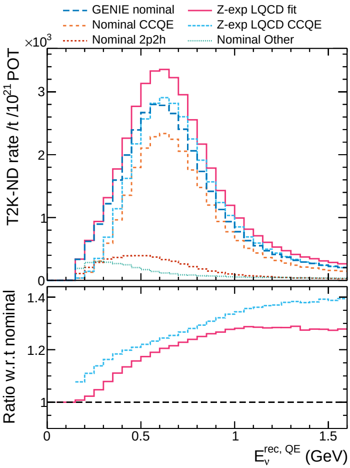

$\nu_\mu - H_2O$ CC0π event rates at T2K.

GENIE nominal: $G_A(Q^2)$ from a dipole fit with $M_A = 0.941$ GeV to νH and νD data.

CC-2p2h, charged-current interaction with two nucleons.

$\tilde{G}_P$ at the muon capture point: g_P^*

$\tilde{G}_P$ not well known from expt: muon capture $\mu^- p \to \nu_\mu n$ gives

$g_P^* = \frac{m_\mu}{2m_N} \tilde{G}_P(Q^2 = 0.88\, m_\mu^2) = 8.06(55)$ [MuCap,1210.6545]

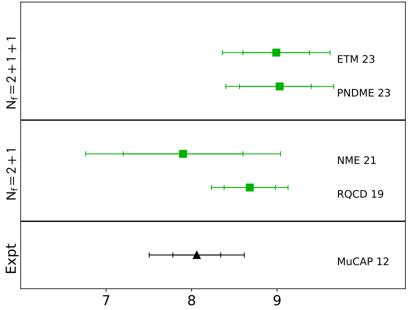

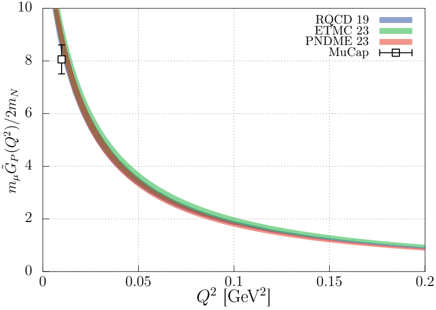

PCAC relation

$$\mathbf{r_{PCAC}} = \frac{m_q G_P(Q^2) + \frac{Q^2}{4m_N}\tilde{G}_P(Q^2)}{m_N G_A(Q^2)} = 1$$

[RQCD,1911.13150] continuum limit.

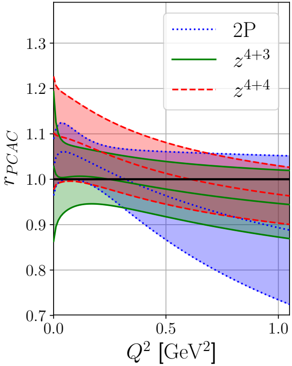

[PNDME,2305.11330]

$\mathbf{r_{PCAC}} = 1 + O(a)$

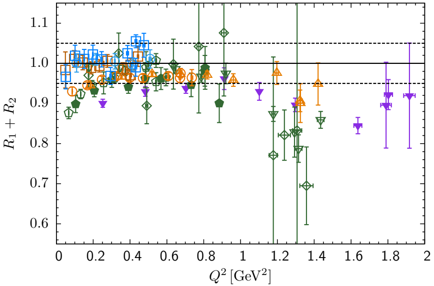

Enhanced excited state contributions ($N \to N\pi$) to G_P and $\tilde{G}_P$. Earlier results saw PCAC relation violated by 40% at M_π^{phys} and $Q^2 = 0.05$ GeV^2 [Jang et al.,1905.06470].

Pion pole dominance

Compare $\tilde{F}_P(Q^2) = \tilde{G}_P(Q^2)\frac{(Q^2+M_\pi^2)}{4m_N^2}$ with $G_A(Q^2)$.

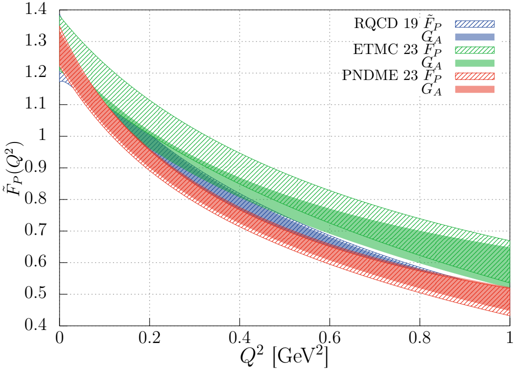

RQCD19: violations of PPD smaller than 2% at $Q^2 = 0$ and smaller than 1% at $Q^2 = 0.5$ GeV^2.

MuCap g_P^* also compatible with pion pole dominance.

$g_{\pi NN}$

This work: [ETMC,2309.05774]

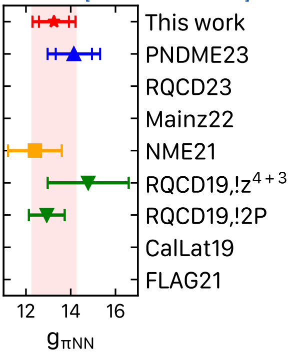

$F_\pi M_\pi^2 g_{\pi NN}$ **at** $M_\pi = M_\pi^{phys}$.

$$\lim_{Q^2 \to -M_\pi^2} (Q^2 + M_\pi^2) m_q G_P(Q^2) = F_\pi M_\pi^2 g_{\pi NN}$$

Also extracted from (assuming PPD):

$$\lim_{Q^2 \to -M_\pi^2} (Q^2 + M_\pi^2) \tilde{G}_P(Q^2) = 4 m_N F_\pi g_{\pi NN}$$

Strange EM and axial form factors

Parity violating *ep* scattering experiments: interference between scattering via γ and Z.

Schlimme Wed 10:45. [P2 expt,1802.04759] Measure the weak charge of the proton $Q_W(p)$.

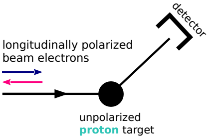

$$A_{PV} = \frac{\sigma^+ - \sigma^-}{\sigma^+ + \sigma^-} = \frac{G_F Q^2}{4\sqrt{2}\pi\alpha_{em}}(Q_W(p) - \boldsymbol{F(E_i, Q^2)})$$

electroweak mixing angle $\sin^2\theta_W \approx (1 - Q_W(p))/4$.

Relevant form factor $\boldsymbol{F(E_i, Q^2)} = F^{EM}(E_i, Q^2) + F^A(E_i, Q^2) + \boldsymbol{F^S(E_i, Q^2)}$.

$F^{EM} \to G^p_{E,M}$, $\quad F^A \to G^p_{E,M}$, $(1 - 4\sin^2\theta_W)G_A^{p,Z}$ $\quad \boldsymbol{F^S} \to G^p_{E,M}$, $G^s_{E,M}$

Estimates of $G^s_{E,M}$ from PV experiments, SAMPLE, A4, HAPPEX and G0.

$G_A^{p,Z} = G_A^s - G_A$,

G_A^s can be constrained by $\nu N \to \nu N$, $\bar{\nu} N \to \bar{\nu} N$ scattering.

μBooNE aims to extract G_A^s in range $Q^2 = 0.08 - 1$ GeV^2.

Strange EM and axial form factors: $G^s_{E,M}$, $G^s_{A,\tilde{P}}$

[ETMC,1909.10744] $M_\pi = 139$ MeV, $a = 0.08$ fm, $LM_\pi = 3.6$.

$G^s_E(Q^2)$

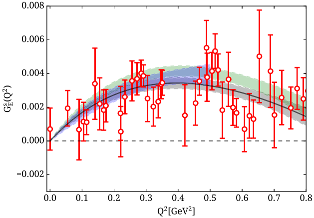

$G^s_M(Q^2)$

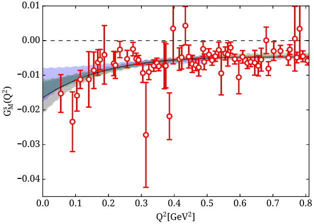

[ETMC,2106.13468] $M_\pi = 139$ MeV, $a = 0.08$ fm, $LM_\pi = 3.6$.

$G^s_A(Q^2)$

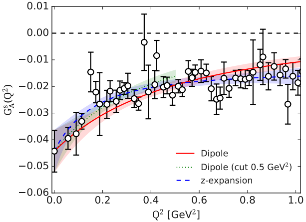

$\tilde{G}^s_P(Q^2)$

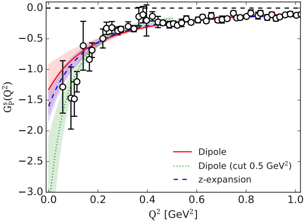

Strange EM and axial form factors: $G^s_{E,M}$, $G^s_{A,\tilde{P}}$

Strange EM form factors: also [Mainz,1903.12566], [χQCD,1705.05849], [LHPC,1505.01803].

[ETMC,1909.10744]

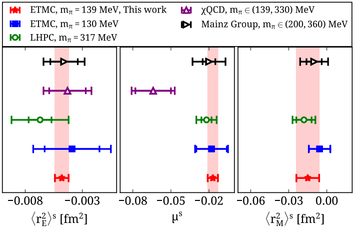

[Mainz,1903.12566], Expt [Maas and Paschke,2017]

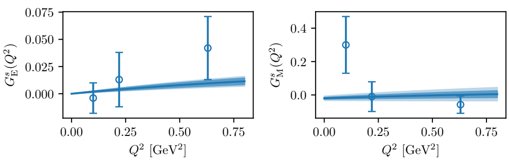

Charm EM form factors: [χQCD,2003.01078]:

$\langle r_E^2 \rangle^c = -0.0005(1)\ \text{fm}^2$, $\mu_M^c = -0.00127(38)\text{stat}\ (5)\text{sys}$, $\langle r_M^2 \rangle^c = -0.0003(1)\ \text{fm}^2$.

Strange and charm axial form factors: [ETMC,2106.13468]:

$\langle r_A^2 \rangle^{1/2,s} = 0.984(239)(12)(295)$ fm, $\langle r_A^2 \rangle^{1/2,c} = 0.987(133)(293)(226)$ fm

see also, e.g., [LHPC,1703.06703].

Summary and outlook

Significant progress has been made in the last few years in the determination of the electromagnetic and axial form factors on the lattice.

- ⋆ First calculation of $G_{E,M}^{p,n}$ where disconnected contributions are included and all sources of systematic uncertainty are considered.
- ⋆ General agreement between results for $G_A(Q^2)$ and $\tilde{G}_P(Q^2)$ over the range $Q^2 = 0 - 1$ GeV^2, after continuum, quark mass, volume extrapolations.

  A number of checks have been passed: consistency with expt. values for g_A and g_P^*. The PCAC relation is satisfied.

  Pion pole dominance is satisfied within the uncertainties at M_π^{phys}.
- ⋆ New results for the strange form factors $G_{E,M}^s(Q^2)$ and $G_{A,P}^s(Q^2)$ and even for charm.

Further studies expected in the next 2-3 years. In the future:

- ⋆ First steps towards computing $N \to N\pi$ matrix elements relevant for $N \to \Delta$, ... transitions have been made. Work on this will continue. The finite volume formalism needs to be implemented.
- ⋆ Investigations of multi-particle excited state contamination to $N \to N$ transitions using a large basis of operators, $N\pi$, $N\pi\pi$, ... and the variational method (GEVP).

Generalised form factors, including the gravitational form factors are also being actively studied.